AMRC-R-389

IMPROVED TREATMENT OF MULTIPLE SCATTERING OF INTENSE CHARGED PARTICLE BEAMS

T. P. Hughes
B. B. Godfrey

July 1982

Prepared for: Defense Advanced Research Projects Agency
Directed Energy Office
Arlington, Virginia 22209

Under Contract: N60921-82-C-0004, Monitored by:
Naval Surface Weapons Center
Silver Spring, Maryland 20910

Prepared by: MISSION RESEARCH CORPORATION
1720 Randolph Road, S.E.
Albuquerque, New Mexico 87106

SECURITY CLASSIFICATION OF THIS PAGE (When Data Entered)

REPORT DOCUMENTATION PAGE		READ INSTRUCTIONS BEFORE COMPLETING FORM
1. REPORT NUMBER	2. GOVT ACCESSION NO. AD-A118299	3. RECIPIENT'S CATALOG NUMBER
4. TITLE (and Subtitle) SMALL ANGLE MULTIPLE SCATTERING OF CHARGED PARTICLE BEAMS		5. TYPE OF REPORT & PERIOD COVERED INTERIM
		6. PERFORMING ORG. REPORT NUMBER AMRC-R-389
7. AUTHOR(s) T. P. Hughes, B. B. Godfrey		8. CONTRACT OR GRANT NUMBER(s) N60921-82-C-00004
9. PERFORMING ORGANIZATION NAME AND ADDRESS MISSION RESEARCH CORPORATION 1720 Randolph Rd., S.E. Albuquerque, New Mexico 87106		10. PROGRAM ELEMENT, PROJECT, TASK AREA & WORK UNIT NUMBERS
11. CONTROLLING OFFICE NAME AND ADDRESS Defense Advanced Research Projects Agency 800 North Quincy Street Arlington, VA 22209		12. REPORT DATE July 1982
		13. NUMBER OF PAGES 29
14. MONITORING AGENCY NAME & ADDRESS(if different from Controlling Office) Naval Surface Weapons Center White Oak Silver Spring, MD 20910		15. SECURITY CLASS. (of this report) UNCLASSIFIED
		15a. DECLASSIFICATION DOWNGRADING SCHEDULE

16. DISTRIBUTION STATEMENT (of this Report)

APPROVED FOR PUBLIC RELEASE - DISTRIBUTION UNLIMITED

17. DISTRIBUTION STATEMENT (of the abstract entered in Block 20, if different from Report)

18. SUPPLEMENTARY NOTES

This work was supported by the Defense Advanced Research Projects Agency (DoD) under ARPA Order No. 4395.

19. KEY WORDS (Continue on reverse side if necessary and identify by block number)

Relativistic electron beams
Multiple scattering
Nordsieck expansion

20. ABSTRACT (Continue on reverse side if necessary and identify by block number)

The scattering of self-pinched particle beams propagating in gas is investigated using Moliere's treatment of multiple scattering. Nordsieck lengths significantly longer than those predicted on the basis of less accurate scattering formalisms are obtained numerically. An improved analytic - expression for the Nordsieck length is derived and agrees well with the numerical results. Experimental data on the beam expansion from the PHERMEX and ASTRON experiments show good agreement with numerical simulations and analytic results. The evolution of a thin annular beam due to scattering is

DD FORM 1 JAN 73 1473 EDITION OF 1 NOV 65 IS OBSOLETE

SECURITY CLASSIFICATION OF THIS PAGE (When Data Entered)

studied and the beam is found to acquire a Bennett profile in a distance on the order of one Nordsieck length.

ABSTRACT

The scattering of self-pinched particle beams propagating in gas is investigated using Moliere's treatment of multiple scattering. Nordsieck lengths significantly longer than those predicted on the basis of less accurate scattering formalisms are obtained numerically. An improved analytic expression for the Nordsieck length is derived and agrees well with the numerical results. Experimental data on beam expansion from the PHERMEX and ASTRON experiments show good agreement with numerical simulations and analytic results. The evolution of a thin annular beam due to scattering is studied and the beam is found to acquire a Bennett profile in a distance on the order of one Nordsieck length.

CONTENTS

Section		Page
	ABSTRACT	i
I	INTRODUCTION	1
II	THEORY OF MULTIPLE SMALL ANGLE SCATTERING	2
III	SCATTERING OF BENNETT-PROFILE BEAMS	9
IV	COMPARISONS WITH EXPERIMENTS	14
V	EVOLUTION OF AN ANNULAR BEAM	15
VI	SUMMARY AND CONCLUSIONS	16
	REFERENCES	17

LIST OF ILLUSTRATIONS

Figure		Page
1	Illustration of disparity between the Moliere and Rossi-Greisen predictions for the mean square transverse momentum of a beam of noninteracting particles as a function of propagation length.	18
2	The shape of the Moliere distribution relative to the Rossi-Greisen Gaussian changes as a function of propagation distance because the value of the parameter B is a function of the latter (noninteracting particles assumed).	19
3	Evolution of a Bennett equilibrium beam. Part (a) shows the exponential increase of the mean radius as a function of propagation distance. Parts (b) and (c) show plots of the transverse momentum distribution function and current density after three Nordsieck lengths of propagation.	20
4	Nordsieck length as a function of beam power. Over a wide range of power the Nordsieck length obtained from SCATR is significantly larger than that obtained from Eq. (7) using the Rossi-Greisen θ_{max}. The implication for some particular electron beams is indicated.	21
5	Experimental data on beam expansion from PHERMEX (black dots) compared to predicted Nordsieck expansion.	22
6	Experimental results from ASTRON compared to SCATR simulations. The ratio of the beam radius 2 m from injection into the gas to the initial radius is plotted as a function of background gas pressure.	23
7	Thin annular rotating beam equilibrium at $\ell = 0$. Parts (a) and (b) are radial profiles of the current density and magnetic field, respectively, while part (c) shows the transverse momentum distribution function.	24
8	Evolution of the annular beam in Fig. 7 due to small angle scattering, showing the development of a Bennett profile.	25

I. INTRODUCTION

When a self-pinched particle beam propagates through a gas, it undergoes multiple scattering off background nuclei. As a result, the mean radius of the beam tends to increase and the mean beam density decreases. Recent experiments at Los Alamos National Laboratory (LANL) using the PHERMEX electron beam have called into question standard formulae used to compute the rate of expansion of the beam. In particular, the length for one e-folding in mean radius, the so-called Nordsieck length, was measured to be about a factor of two longer than the theoretical prediction. In this report, we show that this discrepancy is due to inaccurate treatment of small angle multiple scattering. Section II describes a more accurate treatment based on the Moliere formulation of multiple scattering. We show how a numerical algorithm was constructed to implement this improved treatment in a particle simulation code. In Sec. III, we give the results of numerical computations of Nordsieck length as a function of beam power, using a simple particle code SCATR. On the basis of these results, we carry out a semi-analytical derivation of an expression for the Nordsieck length. Section IV compares numerical and analytical results with experimental data for the PHERMEX and ASTRON electron beams. Good agreement is obtained. In Sec. V, we examine the evolution of a non-Bennett equilibrium (an annular beam) and show that it becomes Bennett-like in less than one Nordsieck length. We summarize our conclusions in Sec. VI.

II. THEORY OF MULTIPLE SMALL ANGLE SCATTERING

When a charged particle passes through a medium made up of scattering centers with cross section $\sigma(\Omega)d\Omega$, the number of scattering events which it undergoes in traveling a distance ℓ is

$$N_o = n\ell \int \sigma(\Omega)d\Omega$$

$$= 2\pi n\ell \int_0^\infty \sigma(\theta)\theta d\theta \ , \qquad (1)$$

where n is the number density of scattering centers, and θ is the angular deflection. In writing Eq. (1) we have made the assumption that the net deflection of the incident particle is small (much less than a radian) so that the path of the incident particle is approximately a straight line. We have also assumed that the cross section is azimuthally symmetric. When $N_o \gg 1$, we are in the multiple scattering regime.

A. Fokker-Planck Formalism

To describe the behavior of a large number of incident particles, we use a distribution function $f(\underset{\sim}{r}_\perp, \underset{\sim}{p}_\perp, t)$ where $\underset{\sim}{r}_\perp$, $\underset{\sim}{p}_\perp$ are the transverse phase space coordinates of the beam of particles. The longitudinal motion of the particles is assumed to be given by $z = vt$ where $v \approx c$ is the beam velocity. The distribution function obeys the transport equation

$$\left(\frac{\partial f}{\partial t}\right)_{z=vt} + \frac{\underset{\sim}{p}_\perp}{\gamma m} \cdot \frac{\partial}{\partial \underset{\sim}{r}_\perp} f + \frac{d\underset{\sim}{p}_\perp}{dt} \cdot \frac{\partial}{\partial \underset{\sim}{p}_\perp} f = \left(\frac{\partial f}{\partial t}\right)_{coll}$$

$$\equiv -2\pi nv\, f \int \sigma(\chi)\chi d\chi$$

$$+ 2\pi nv \int f(\underset{\sim}{\theta} - \underset{\sim}{\chi})\, \sigma(\chi)\, d\underset{\sim}{\chi} \qquad (2)$$

where $\frac{dp_\perp}{dt}$ is the force due to self fields, $\underset{\sim}{\theta}$ is a vector in the transverse plane related to $\underset{\sim}{p}_\perp$ by $\theta = \underset{\sim}{p}_\perp/\gamma mc$, m is the electron mass and $\gamma = (1-v^2/c^2)^{-1/2}$. For many purposes, the Fokker-Planck treatment of the collision operator on the right-hand side is adequate. This consists of an expansion to second order in χ yielding

$$\left(\frac{\partial f}{\partial t}\right)_{coll} = \frac{1}{4} \langle \dot{\chi}^2 \rangle \left[\frac{\partial^2 f}{\partial \theta^2} + \frac{1}{\theta} \frac{\partial f}{\partial \theta}\right] \tag{3}$$

where

$$\langle \dot{\chi}^2 \rangle = 2\pi n v \int_0^\infty \chi^3 \, d\chi \, \sigma(\chi)$$

The small angle Rutherford cross section for an electron scattering off a nucleus is

$$2\pi\sigma(\chi)\,\chi d\chi = \frac{8\pi Z(Z+1)}{\beta^4\gamma^2}\left(\frac{e^2}{mc^2}\right)^2 \frac{\chi d\chi}{\chi^4}$$

$$\equiv 2\alpha^2 \chi d\chi/\chi^4 \tag{4}$$

where -e is the electron charge, Ze the nuclear charge, and $\beta = v/c$. Substituting this into Eq. (3), we find that the integral for $\langle \dot{\chi}^2 \rangle$ is improper at both the lower and upper limits of integration. The divergence at the lower limit is due to the long range of the bare Coulomb potential. A suitable cutoff can be introduced by taking account of the screening effect of atomic electrons. For the Thomas-Fermi atomic model, for example, one obtains[1] the lower bound $\theta_{min} = \lambda\!\!\!^{-}/a \equiv \lambda\!\!\!^{-}/(0.855 a_0 Z^{-1/3})$ where $\lambda\!\!\!^{-}$ is the deBroglie wavelength of the incident electron, and a_0 is the Bohr atomic radius.

The divergence at the upper limit is an artifact of the small angle approximation used, since a particle cannot scatter through an angle greater than π. The Fokker-Planck equation can be derived only in the small angle limit, however, so that one can either (a) introduce some reasonable upper bound on the scattering angle or (b) go to a different treatment of small angle scattering. Two commonly used upper bounds are $\theta_{max} = \pi$ for low electron energies ($\gamma < 100$) and $\theta_{max} = \lambda\!\!\!^{-}/R_N$, where R_N is the nuclear radius, used by Rossi and Greisen, for high energies[2] ($\gamma > 100$). Using either of these, one can solve Eq. (2) analytically for certain initial conditions.[1,3] For future reference, we give the results for two cases:

(i) Noninteracting Particles

Assume the incident beam to have infinite radial extent with $\partial/\partial \underset{\sim}{r}_\perp \equiv 0$ and let $f \propto \delta(\underset{\sim}{v}_\perp)$ at $t = 0$. The solution to Eqs. (2) and (3) is then

$$f(\theta,\ell) \propto \exp[-\theta^2/\langle\dot{\chi}^2\rangle\ell] \quad , \tag{5}$$

where $\ell = vt$. Since $\langle\dot{\chi}^2\rangle = 2n\alpha^2\, \ell n(\theta_{max}/\theta_{min})$ is a constant, the beam acquires a Maxwellian distribution in transverse velocity whose temperature increases linearly with the distance propagated.

(ii) Self-Pinched Bennett-Profile Beam

From Eqs. (2) and (3), Lee[4] has shown that a Bennett equilibrium beam expands self-similarly due to scattering with Bennett radius

$$R(\ell) = R_0 \exp(\ell/L_N) \tag{6}$$

where L_N is the so-called Nordsieck length. Equation (6) is valid as long as $v/L_N \ll \omega_\beta(R)$, where ω_β is the mean betatron frequency, i.e., the beam expansion is quasi-static. The expression obtained for L_N is

$$L_N = \frac{v\gamma}{n\gamma^2\alpha^2 \ell n(\theta_{max}/\theta_{min})} \quad . \tag{7}$$

where ν is Budker's parameter. Here and subsequently, ν is a measure of the net current flowing. The plasma current is assumed to have the same profile as the beam current. Taking $\theta_{max} = \lambda\!\!\!^{-}/R_N$, we obtain $\ell n(\theta_{max}/\theta_{min}) \approx 2\ell n(210Z^{-1/3})$. For $\theta_{max} = \pi$, $\ell n(\theta_{max}/\theta_{min}) = \ell n(192\gamma\beta Z^{-1/3})$. We shall see that these values for θ_{max} overestimate the effect of small angle scattering over a wide range of parameters relevant to present-day beam propagation experiments.

B. Moliere Formalism

For the case of noninteracting particles with $\partial f/\partial \underline{r}_\perp \equiv 0$ and $f(t=0) \propto \delta(\underline{v}_\perp)$, Eq. (2) can be solved exactly for arbitrary $\sigma(\theta)$ by the use of Fourier-Bessel transforms. This was first done by Moliere[5], but the brief description given here is from a simpler derivation of Moliere's equation by Bethe.[1] The solution takes the form

$$f(\theta,t) = \int_0^\infty \eta \, d\eta \, J_0(\eta\theta) \, e^{N(\eta) - N_0} \quad , \tag{8a}$$

where $N(\eta) = n\ell \int_0^\infty \sigma(\chi) J_0(\eta\chi) \, \chi \, d\chi$, (8b)

and J_0 is the Bessel function of order zero.

When $N_0 \gg 1$, only values of η for which $N_0 - N(\eta) \ll N_0$ contribute in Eq. (8a). For this regime, it turns out that Eq. (8b) can be evaluated analytically. To do this most conveniently, one changes variable to $\xi = \eta(n\ell\alpha^2 B)^{1/2}$, where B is the solution to

$$e^B/B = n\ell\alpha^2/(1.32\theta_{min}^2) = N_0/1.32 \quad . \tag{9}$$

Then one can write

$$N(\xi) - N_0 = -\frac{\xi^2}{4} + \frac{\xi^2}{4B} \ell n \frac{\xi^2}{4} \tag{10}$$

for $0 < \xi < B^{1/2}$. Substituting this into Eq. (8a), one obtains Moliere's expansion in 1/B:

$$f(\theta)\theta d\theta = \zeta d\zeta[f^{(0)}(\zeta) + B^{-1} f^{(1)}(\zeta) + B^{-2} f^{(2)}(\zeta) + \ldots] \tag{11}$$

where $\zeta = \theta/(n\ell\alpha^2 B)^{1/2}$, and $f^{(0)} = \exp(-\zeta^2)$. Thus, the leading term in the Moliere expansion is a Gaussian of width $\theta_M \equiv (n\ell a^2 B)^{1/2}$. When B is large (> 10) we can write $B \approx \ell n\ N_0 \propto \ell n(\ell)$. So, in contrast to the result in Eq. (5), we find that the transverse temperature of the beam increases as $\ell\ \ell n(\ell)$ instead of as ℓ.

Comparing the widths of the Gaussians from Eqs. (5) and (11), we find that Eq. (5) overestimates the mean square transverse momentum of a beam of noninteracting particles propagating in air (see Fig. 1). Because the width of the Moliere Gaussian increases faster than linearly with ℓ, it eventually catches up to the Rossi-Greisen value, but only after ~ 10^4 meter-atmospheres.

Having derived the Moliere result, one can go back and deduce what value one should use for θ_{max} to obtain the Moliere Gaussian width. One finds that $\theta_{max} = \theta_M$ is the appropriate cutoff, i.e.,

$$\chi^2\ \ell \equiv \theta_M^2 = 2\pi n\ell \int_{\theta_{min}}^{\theta_M} \chi^3 d\chi\ \sigma(\chi) \tag{12}$$

This leads to a transcendental equation for θ_M which is equivalent to Eq. (9). The main effect of the higher order terms in Eq. (11) is to produce a long tail on the distribution. For large values of ζ, the expression for f goes over to the Rutherford single scattering form. As a result of this tail on the distribution function, one finds that the shape of the distribution function changes as a function of propagation distance, as shown in Fig. 2. The greater the propagation distance, the closer the distribution approaches the Rossi-Greisen Gaussian, and the smaller the percentage of particles in the tail.

When self-field effects are retained, Eq. (2) becomes rather intractable. Analysis along the lines of Ref. 4 is made difficult by the fact that the rate of transfer of energy to the transverse direction is not constant, but depends on the scattered state of the beam. In Sec. III we show, however, that a semi-analytical treatment can be performed for the special case of a Bennett equilibrium.

C. Numerical Algorithm

In order to look at problems where self-fields are important, we devised a numerical algorithm to implement Moliere scattering in particle simulation codes. In the algorithm, scattering angles are picked randomly from a Moliere distribution. The distribution used is one corresponding to a distance of propagation $\Delta\ell$ much less than the characteristic length over which the beam radius changes due to scattering. To compute the Moliere distribution one has to perform time-consuming numerical integrations, so we divide the distribution into two parts,

$$P(\zeta)\, d\zeta = \begin{cases} f(\zeta)\, \zeta d\zeta & \zeta < \zeta_{cut} \\ \dfrac{2}{B}\, \dfrac{\zeta d\zeta}{\zeta^4} & \zeta > \zeta_{cut} \end{cases} \qquad (13)$$

where ζ_{cut} is an angle at which the Rutherford expression becomes a good approximation to the exact Moliere expression. At $\zeta_{cut} = 6$, for example, the discrepancy between the two expressions is 15%. For $\zeta < \zeta_{cut}$, an array of scattering angles is computed once and for all on the first pass through the algorithm. For $\zeta > \zeta_{cut}$, scattering angles can be obtained directly from an analytic expression, and it is thus not too time-consuming to generate new angles each time a scattering is required, especially since large angle scatterings are relatively rare. The actual choice of a scattering angle proceeds as follows. A random number X is chosen between 0 and A where $A = \int P(\zeta)d\zeta$. If $X < A_M$, where $A_M = \int P(\zeta)d\zeta$ then the angle corresponding to X is obtained from the permanent array. If $X > A_M$, the corresponding angle is computed analytically.

The length $\Delta\ell$ cannot be made arbitrarily small, because Moliere theory breaks down rapidly for $N_0(\Delta\ell) < 20$. To avoid some numerical integration problems, we generally choose $\Delta\ell$ such that $N_0 \geq 40$ in our algorithm. When a beam expands to the point where $\omega_\beta \sim v/L_N$, this value of $\Delta\ell$ can become comparable to the length scale over which the beam radius changes (see Sec. IVB). We then resort to the treatment of Keil, Zeitler, and Zinn[6,7] which is specifically addressed to the regime $1 \leq N_0 \leq 20$, the so-called "plural" scattering regime. We can thus chose a suitably small $\Delta\ell$ while maintaining accuracy.

III. SCATTERING OF BENNETT-PROFILE BEAMS

A. Preservation of Bennett Profile

On the basis of a Fokker-Planck treatment of scattering, Lee[4] has shown that the Bennett equilibrium is a self-similar solution to Eq. (2) with the Bennett radius obeying the Nordsieck equation, Eq. (6). It is desirable to know if this important result carries through when Moliere scattering is employed. To answer this, we inserted the scattering algorithm described in Sec. II into the one-dimensional particle simulation code SCATR. SCATR simulates the behavior of an infinitely long, axisymmetric self-pinched beam in the high-energy paraxial approximation ($v = c$, $\nu/\gamma \ll 1$). The equations which SCATR solves are (1) the Lorentz equations for the transverse motion of the individual particles and (2) Ampere's law for the self-magnetic field.

The results of simulating a 10 kA, 50 MeV beam with an initial Bennett radius of 0.5 cm are shown in Fig. 3. In Fig. 3(a) the mean radius (the radius enclosing half of the total current) is plotted, and is seen to e-fold about three times during the run. The fact that the plotted line is straight means that the radius is growing exponentially with a constant Nordsieck length L_N. In the Fokker-Planck treatment of Eq. (2), this behavior is predicted due to the facts that (1) energy is scattered into the transverse direction at a constant rate and (2) the scattered distribution is Gaussian. The numerical results suggest that these conditions are at least approximately fulfilled when Moliere scattering is applied. In Fig. 3(b) we compare the transverse distribution functions of the beam, after it has propagated three Nordsieck lengths, with an exact Gaussian. The agreement is good except in the tail. Initially, the distribution functions is exactly Gaussian, as required for a Bennett equilibrium, and the non-Gaussian tail is observed to grow slowly. At the stage reached in Fig. 3, however, it appears to have no effect on the spatial current

distribution, shown in Fig. 3(c). It seems reasonable to assume that the tail will have little practical significance for beam propagation: it grows up so slowly that the beam will have expanded to very large radius by the time a significant number of particle reside in the tail. As the radius increases, the confining magnetic field weakens and the state of quasi-static equilibrium disappears, allowing the particles to freely expand.

The presence of the long Rutherford tail on the scattering distribution has another noteworthy effect. A non-negligible number of particles undergo large angle scatterings which kick them clear of the beam. If a particle reaching a radial position greater than ten Bennett radii is considered lost from the beam, we find that 2-3% of the beam current is lost per Nordsieck length. This loss rate is, of course, negligible for practical purposes.

B. Evaluation of Nordsieck Lengths

Equation (7) shows that for a Bennett beam, the Nordsieck length as usually defined depends only on the beam power $\nu\gamma$ (since $\gamma^2\alpha^2$ is a constant). Using SCATR we have found this to be the case with Moliere scattering also. The Nordsieck lengths obtained from SCATR are compared to those from Eq. (7) in Fig. 4. The Rossi-Greisen value for θ_{max} was used in Eq. (7). The implications for some present-day beam machines are shown: for PHERMEX, the SCATR Nordsieck length is twice as long as that predicted by Eq. (7); for ATA, the SCATR length is 40% longer than the Eq. (7) result. When $\nu\gamma$ reaches a value of 10^4, there is little difference between the SCATR and Rossi-Greisen results. Despite appearances, the SCATR Nordsieck length is not exactly linear in $\nu\gamma$ (see following subsection).

C. Analytic Expression for Nordsieck Length

The envelope equation for a self-pinched beam[3] yields a general expression for the Nordsieck length,

$$L_N = \frac{2v\gamma m^2 c^3}{\left\langle \frac{dp_\perp}{dt}^2 \right\rangle} , \tag{14}$$

where $\langle dp_\perp^2/dt \rangle$ is the rate at which the mean square transverse momentum of the beam changes due to scattering. As noted in subsection A, Moliere scattering yields (1) an approximately constant value for $\langle dp_\perp^2/dt \rangle$ and (2) an approximately Gaussian distribution in transverse momentum. Thus, to compute the value of $\langle dp_\perp^2/dt \rangle$, we throw away the non-Gaussian corrections in Moliere's Eq. (11). We obtain,

$$\frac{1}{m^2c^2} \left\langle \frac{dp_\perp^2}{dt} \right\rangle = \gamma^2 \frac{d\theta_M^2}{dt} = n\gamma^2\alpha^2 \left(vB + vt \frac{dB}{dt}\right) \tag{15}$$

From Eq. (9) we obtain

$$\frac{dB}{dt} = \frac{1}{t} \frac{B}{(B - 1)} \tag{16}$$

Substituting Eqs. (15) and (16) into Eq. (14), we obtain

$$L_N = \frac{2v\gamma (B - 1)}{n\gamma^2\alpha^2B^2} \tag{17}$$

The parameter B is a function of the transverse beam temperature, which tends to remain constant during quasi-static expansion of the beam.[4] This is because the increase in transverse energy due to scattering is balanced by the work done in expanding against the magnetic field. To compute B we use the expression for the transverse temperature of a Bennett beam, i.e., $v_{th}^2 = v/\gamma$, where v_{th} is the thermal velocity, so that

$$n\ell\alpha^2 B = \nu\gamma \tag{18}$$

combining this with Eq. (9), we obtain

$$B = \ell n(\nu\gamma/1.32\gamma^2\theta^2_{min}) \tag{19}$$

Substitution into Eq. (17) gives

$$L_N = \frac{2\nu\gamma[\ell n(\nu\gamma/1.32\gamma^2\theta^2_{min}) - 1]}{n\gamma^2\alpha^2[\ell n(\nu\gamma/1.32\gamma^2\theta^2_{min})]^2} \tag{20}$$

If one substitutes values for α and n appropriate to air into Eq. (20) one obtains

$$L_N = 7.14\ \nu\gamma\ \frac{\ell n(1090\ \nu\gamma)}{[\ell n(2970\ \nu\gamma)]^2}\ \text{meter-atm}\ . \tag{21}$$

Equation (21) agrees to within 5% with the results of SCATR for $\nu\gamma \gtrsim 50$ and within about 10% for $\nu\gamma \lesssim 50$, as shown in Table 1. The better agreement at larger values of $\nu\gamma$ is to be expected when one considers that corrections to the Gaussian in Moliere's theory enter to order 1/B.

TABLE 1. Comparison of Nordsieck lengths obtained from SCATR with those obtained from Eqs. (21) and (7). The value of the Moliere expansion parameter B used in Eq. (21) is also tabulated.

	Nordsieck Length (meter-atm)			
v_Y	SCATR	Eq. (21)	Eq. (7)	B
0.68 (PHERMEX)	0.59	0.55	0.27	6.6
5.88 (ETA)	3.9	3.9	2.3	8.8
8.0 (PHERMEX UPGRADE)	5.7	5.1	3.1	9.0
58.8 (ATA)	33.4	32	23.2	11.1
588	284	272	232	13.4
5880	2404	2367	2320	15.7

IV. COMPARISONS WITH EXPERIMENTS

A. PHERMEX

Our work on small angle multiple scattering of particle beams originally was undertaken in support of a series of propagation experiments at the PHERMEX electron beam facility at Los Alamos National Laboratory. At present, PHERMEX produces a 200-300 A, 21 MeV beam with a 1 mm diameter beam. This beam was injected into a balloon filled with helium at 580 torr, and the spot size was measured as a function of propagation distance. The results are shown in Fig. 5. The limited data available agrees rather well with the Moliere scattering result. Additional comparisons with PHERMEX will be made early next year at an order-of-magnitude larger beam power.

B. ASTRON

The ASTRON beam at Lawrence Livermore National Laboratory was used in a study of beam expansion due to scattering some years ago.[4,8] In one experiment, the beam was injected into a tank of gas of variable pressure. The beam radius was measured two meters downstream as a function of the gas pressure. Because the ASTRON beam has a low power, it Nordsieck-expands only for a short while and then goes over into the free expansion regime. As a result, when we simulated the experiment using SCATR, we had to use a "plural" scattering algorithm, instead of a multiple scattering algorithm as discussed in Sec. IIC. The experimental results for propagation in nitrogen and argon are compared to the SCATR results in Fig. 6. The agreement is good for both gases, and that for argon is an improvement on the agreement previously reported by Lee.[4] In Refs. 4 and 8, the value of θ_{max} used is that due to Williams[9] and is approximately equal to θ_M (see paragraph following Eq. (11)). However, these two references assume that θ_{max} is a function of propagation distance, which is true for noninteracting particles, but not for a quasi-static self-pinched beam. For the latter, $\theta_{max} = (n\ell a^2 B)^{1/2}$ is a constant, with B given by Eq. (19).

V. EVOLUTION OF AN ANNULAR BEAM

It has been shown by Lee[4] that under certain restrictions a self-pinched beam near equilibrium tends to assume a Bennett profile due to small angle scattering. The rate at which this occurs was not computed, however, and to do so analytically would be laborious. SCATR is a useful tool for addressing this problem. We chose to investigate the evolution of a beam which starts out far from being a Bennett equilibrium viz., a rotating thin annular beam. Like the Bennett profile beams we have previously examined, the beam is assumed to be charge-neutral, nondiamagnetic, and self-pinched. The equilibrium current, magnetic field, and transverse velocity profiles are shown in Fig. 7. The value of $\nu\gamma$ for the beam is 50, which gives a predicted Nordsieck length of 27.5 m-atm in air [from Eq. (21)]. When the beam propagates, we find that it expands slower than the predicted rate for about the first Nordsieck length, and thereafter expands at the predicted rate, as shown in Fig. 8(a). If we look at what is happening to the structure of the beam during this time, we find that its annular shape is rapidly destroyed. Figure 8(b) shows that in less than a Nordsieck length, the beam has completely filled in and its transverse velocity profile is close to being Gaussian. At this point, only the rotation of the beam is preventing the current profile from looking more like a Bennett profile. As the beam expands, the rotation slows down due to conservation of annular momentum and the beam profile becomes very close to being Bennett-like (Fig. 8(c)). On the basis of these results, we think that it is reasonable to assume that any self-pinched high energy beam with low ν/γ will acquire a Bennett profile in a distance on the order of one Nordsieck length.

VI. SUMMARY AND CONCLUSIONS

We have carried out an investigation of multiple small angle scattering of particle beams based on the Moliere equations. Our results for Bennett equilibria obtained from a simple particle simulation code SCATR give Nordsieck lengths significantly longer than those calculated from commonly used expressions based on the less accurate Rossi-Greisen formalism. On the basis of our numerical results, we are able to derive an improved analytic expression for the Nordsieck length which agrees to within 5-10% with the numerical results, depending on the beam power.

We obtain good agreement with experimental data on beam expansion from the PHERMEX and ASTRON electron beams. For PHERMEX we predicted a Nordsieck length which was twice as long as that obtained from a commonly used expression. The experimental evidence supports our result. For the ASTRON data, the agreement is significantly better than that previously obtained by other workers.

Finally, we have studied the evolution of a non-Bennett equilibrium namely, a thin annular beam, under the influence of small angle scattering. In a distance on the order of the Nordsieck length, the beam assumes a Bennett profile in current and a Gaussian distribution in transverse momentum. Based on this example, we tentatively conclude that all self-pinched beam equilibria with $v \approx c$ and $v/\gamma \ll 1$, will evolve to a Bennett distribution in roughly one Nordsieck length.

REFERENCES

1. H. A. Bethe, Phys. Rev. 89, 1256 (1950).

2. B. Rossi and K. Greisen, Rev. Mod. Phys. 13, 240 (1944).

3. E. P. Lee and R. K. Cooper, Part. Accel. 7, 83 (1976).

4. E. P. Lee, Phys. Fluids 19, 61 (1976).

5. G. Moliere, Z. Naturforsch. 3a, 78 (1948).

6. E. Keil, E. Zeitler, and W. Zinn, Z. Naturforsch. 15a 1031 (1960). (A discussion of their work is given in Ref. 7.)

7. W. T. Scott, Rev. Mod. Phys. 35, 231 (1963).

8. R. J. Briggs, R. E. Hester, E. J. Lauer, E. P. Lee, and R. L. Spoerlein, Phys. Fluids 19, 1007 (1976).

9. E. J. Williams, Proc. Roy. Soc. A169, 542 (1939).

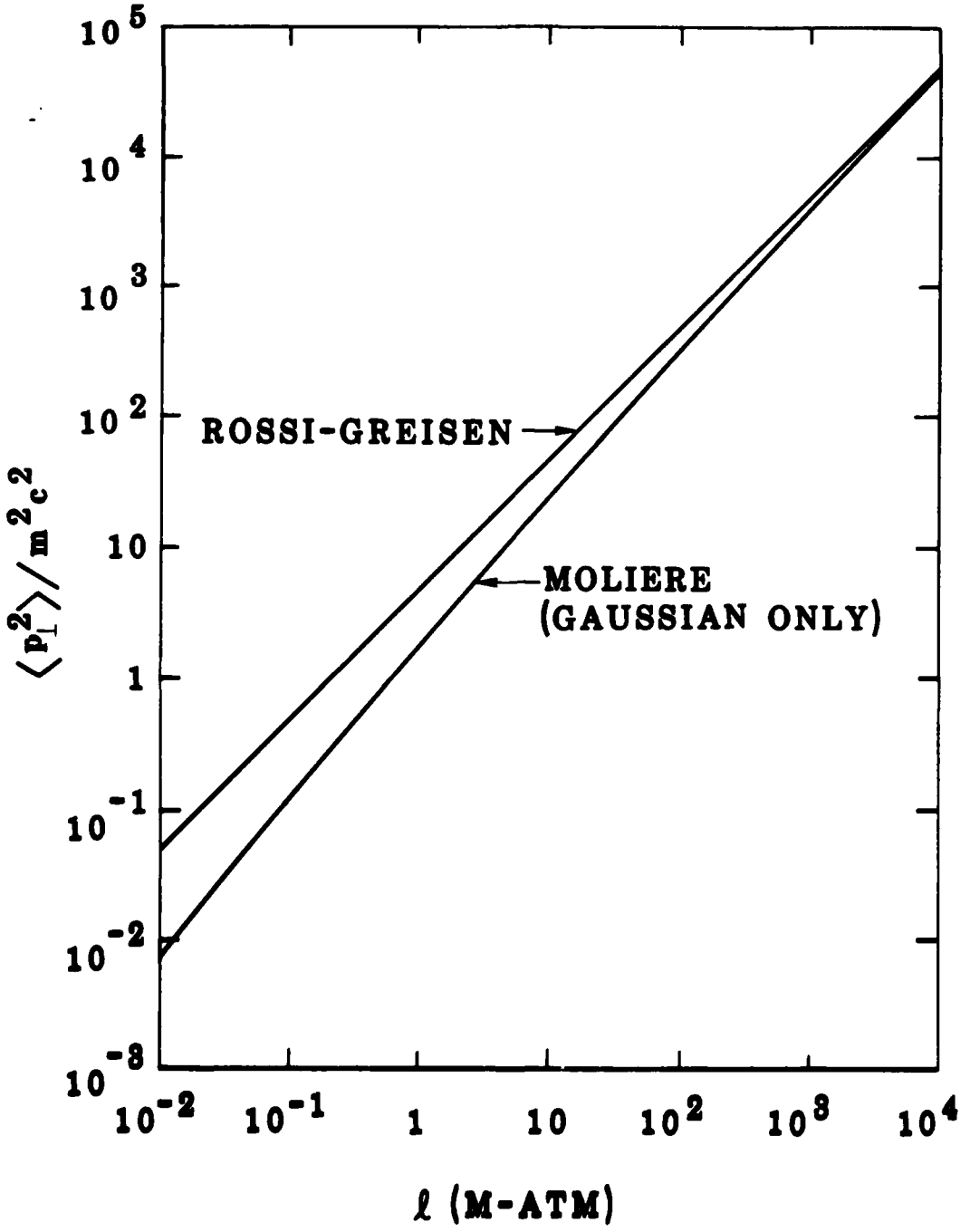

Figure 1. Illustration of disparity between the Moliere and Rossi-Greisen predictions for the mean square transverse momentum of a beam of noninteracting particles as a function of propagation length.

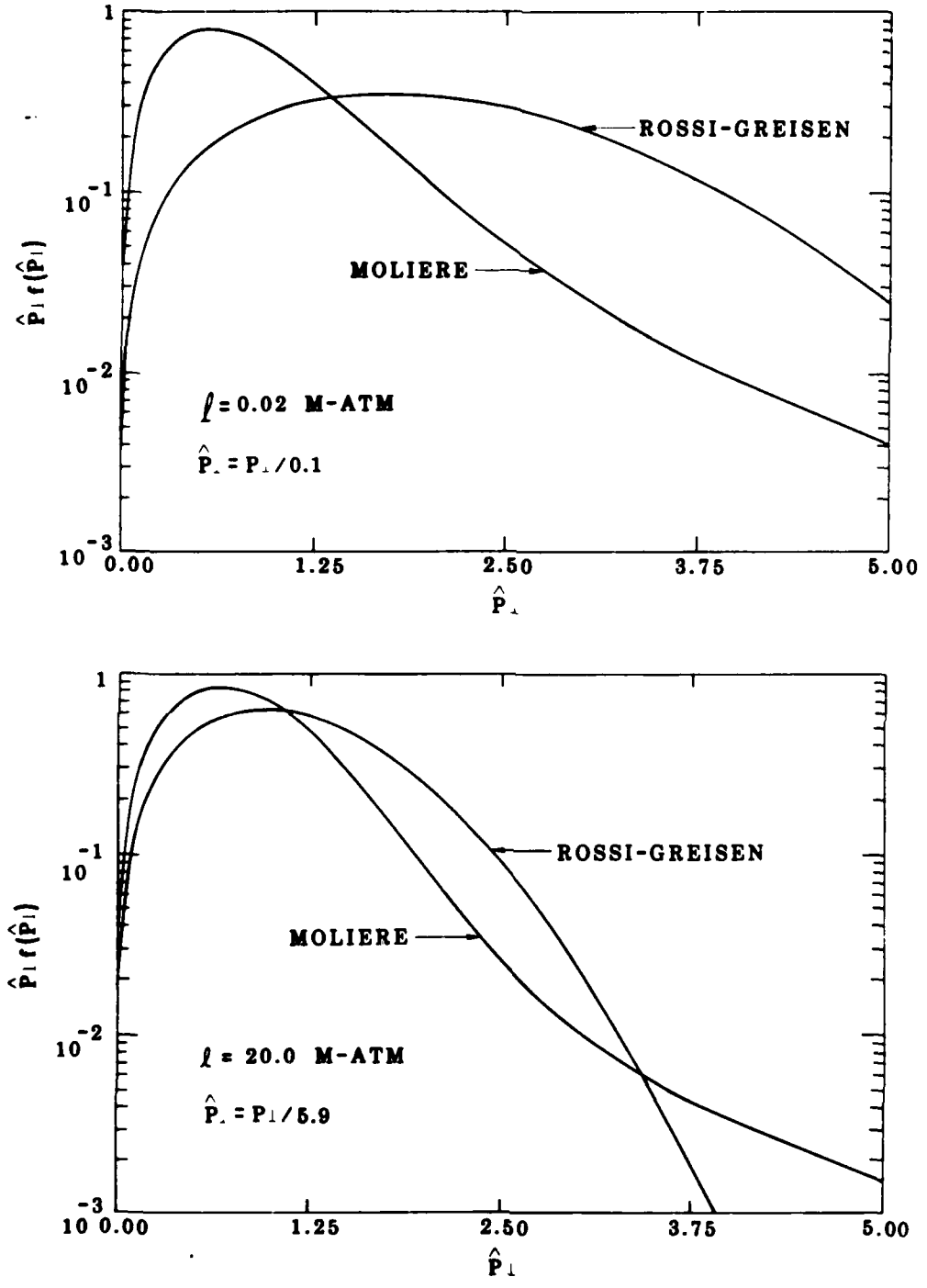

Figure 2. The shape of the Moliere distribution relative to the Rossi-Greisen Gaussian changes as a function of propagation distance because the value of the parameter B is a function of the latter (noninteracting particles assumed).

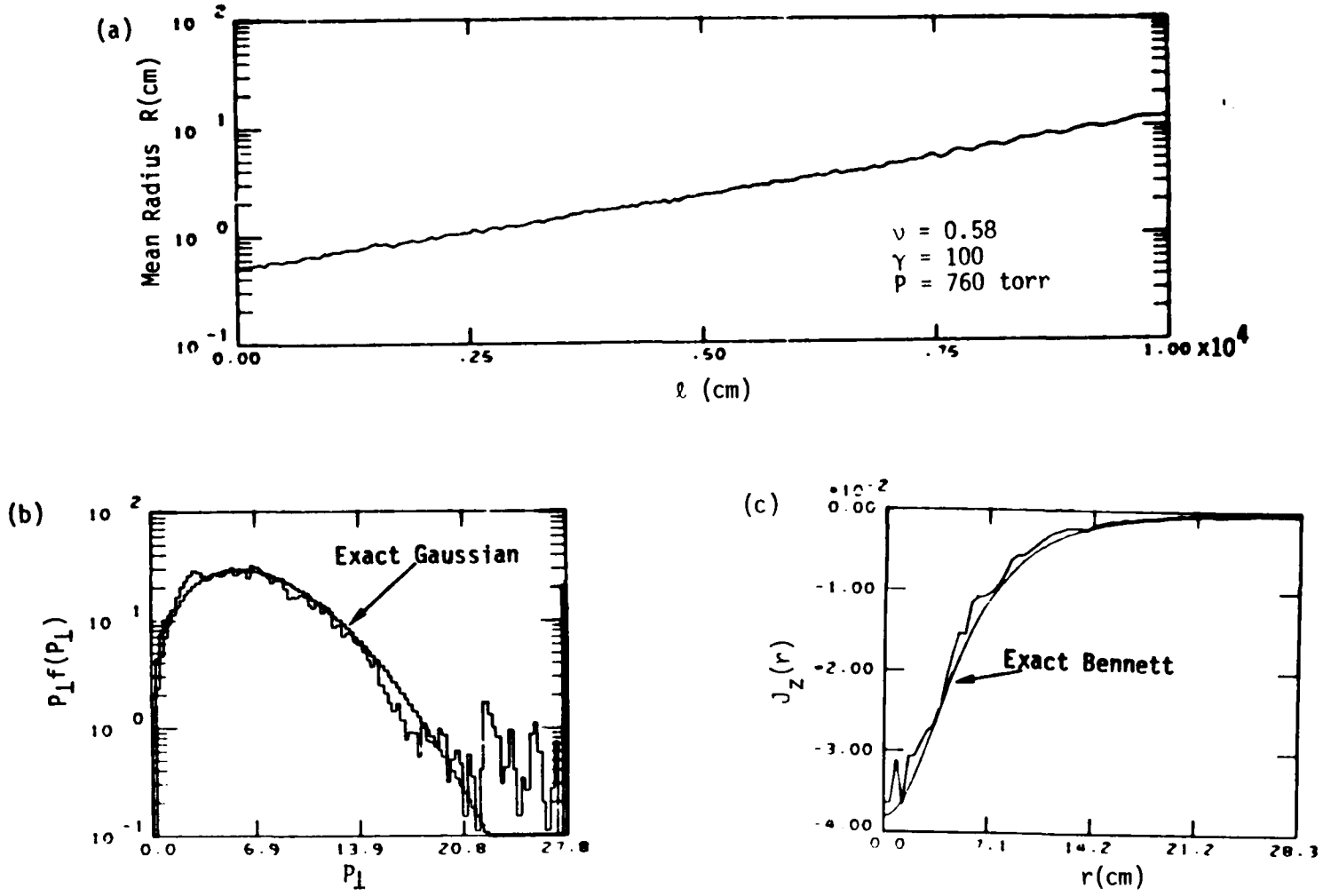

Figure 3. Evolution of a Bennett equilibrium beam. Part (a) shows the exponential increase of the mean radius as a function of propagation distance. Parts (b) and (c) show plots of the transverse momentum distribution function and current density after three Nordsieck lengths of propagation.

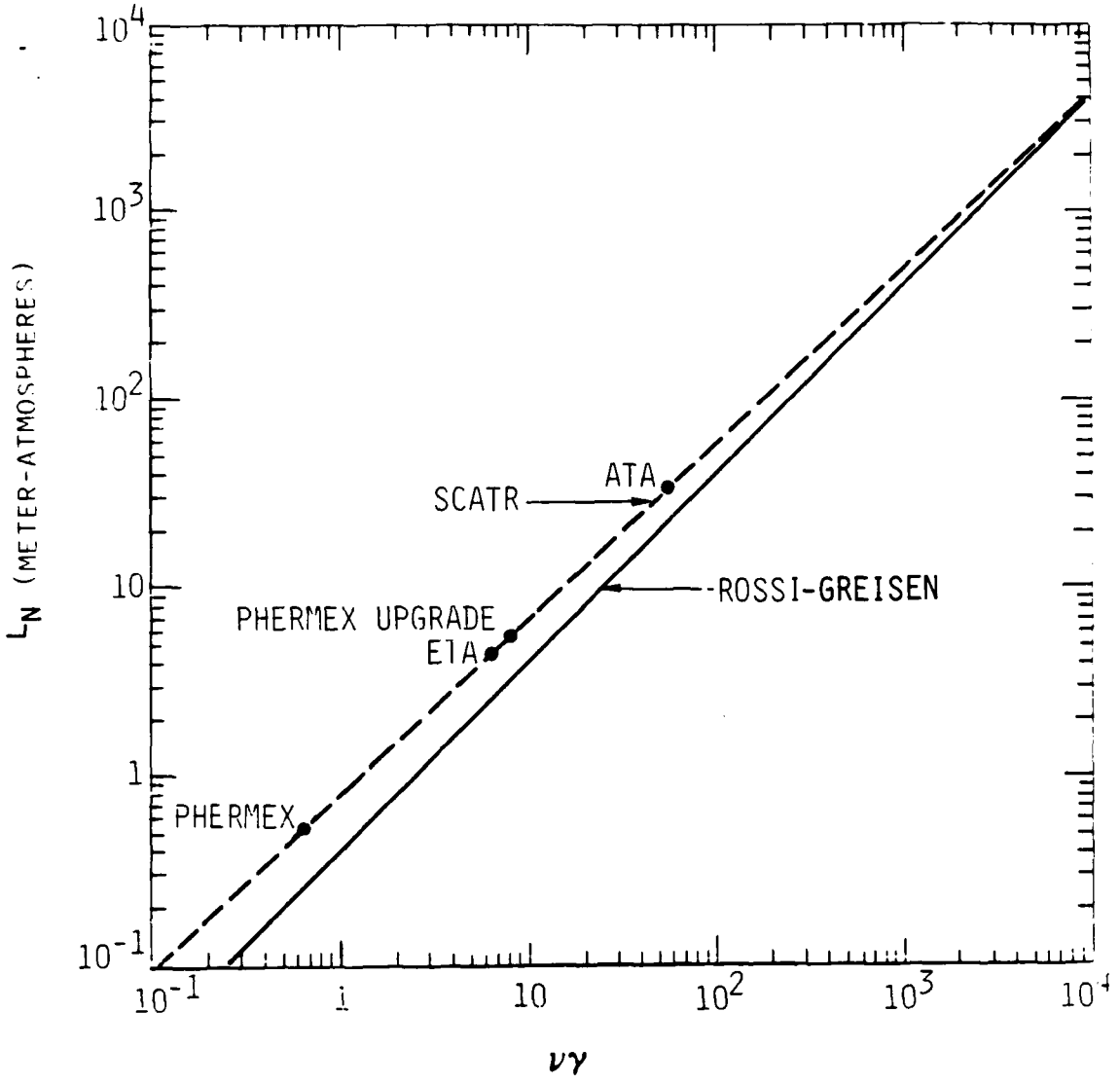

Figure 4. Nordsieck length as a function of beam power. Over a wide range of power the Nordsieck length obtained from SCATR is significantly larger than that obtained from Eq. (7) using the Rossi-Greisen θ_{max}. The implication for some particular electron beams is indicated.

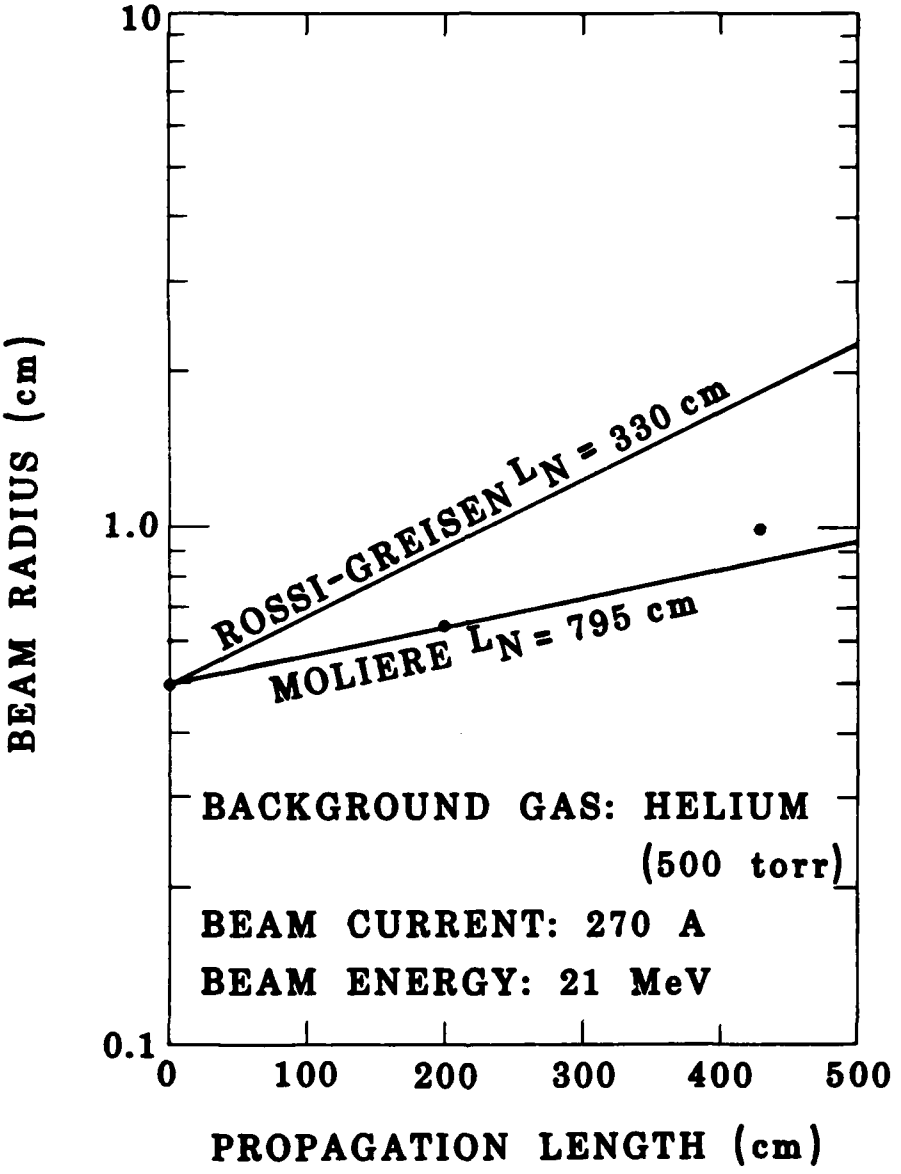

Figure 5. Experimental data on beam expansion from PHERMEX (black dots) compared to predicted Nordsieck expansion.

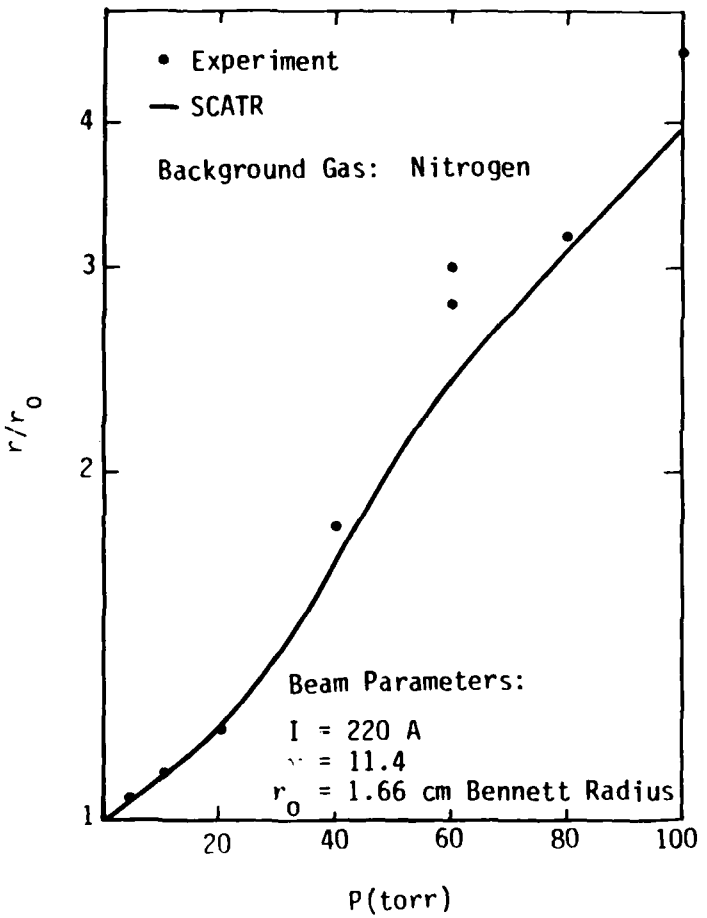

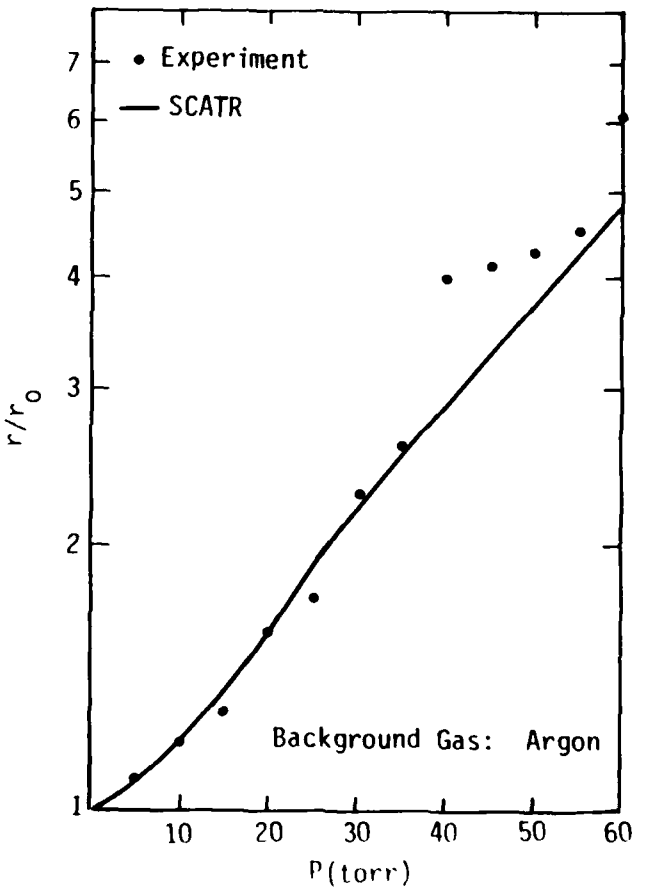

Figure 6. Experimental results from ASTRON compared to SCATR simulations. *The ratio of the beam radius 2 m from injection into the* gas to the initial radius is plotted as a function of background gas pressure.

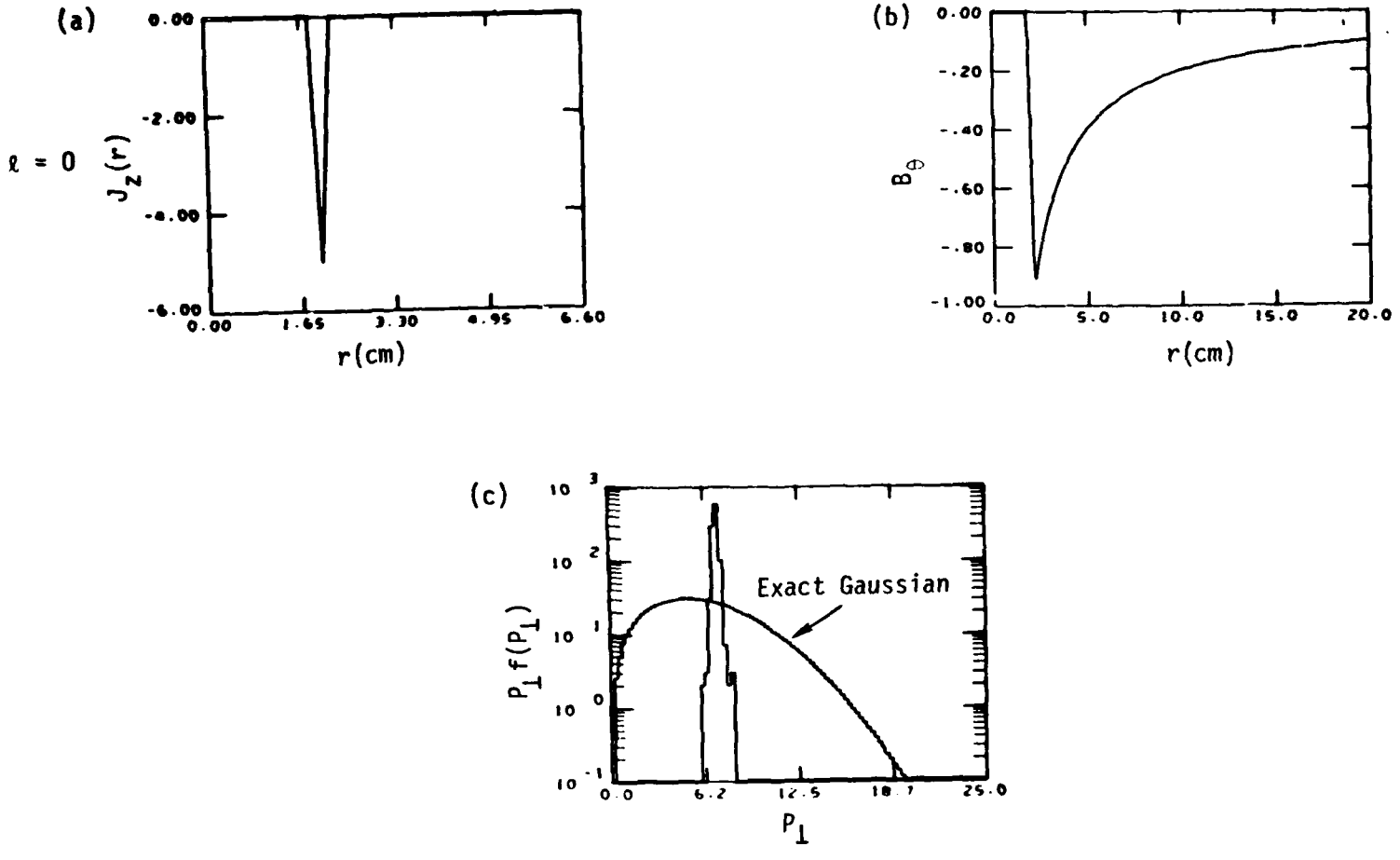

Figure 7. Thin annular rotating beam equilibrium at ℓ = 0. Parts (a) and (b) are radial profiles of the current density and magnetic field, respectively, while part (c) shows the transverse momentum distribution function.

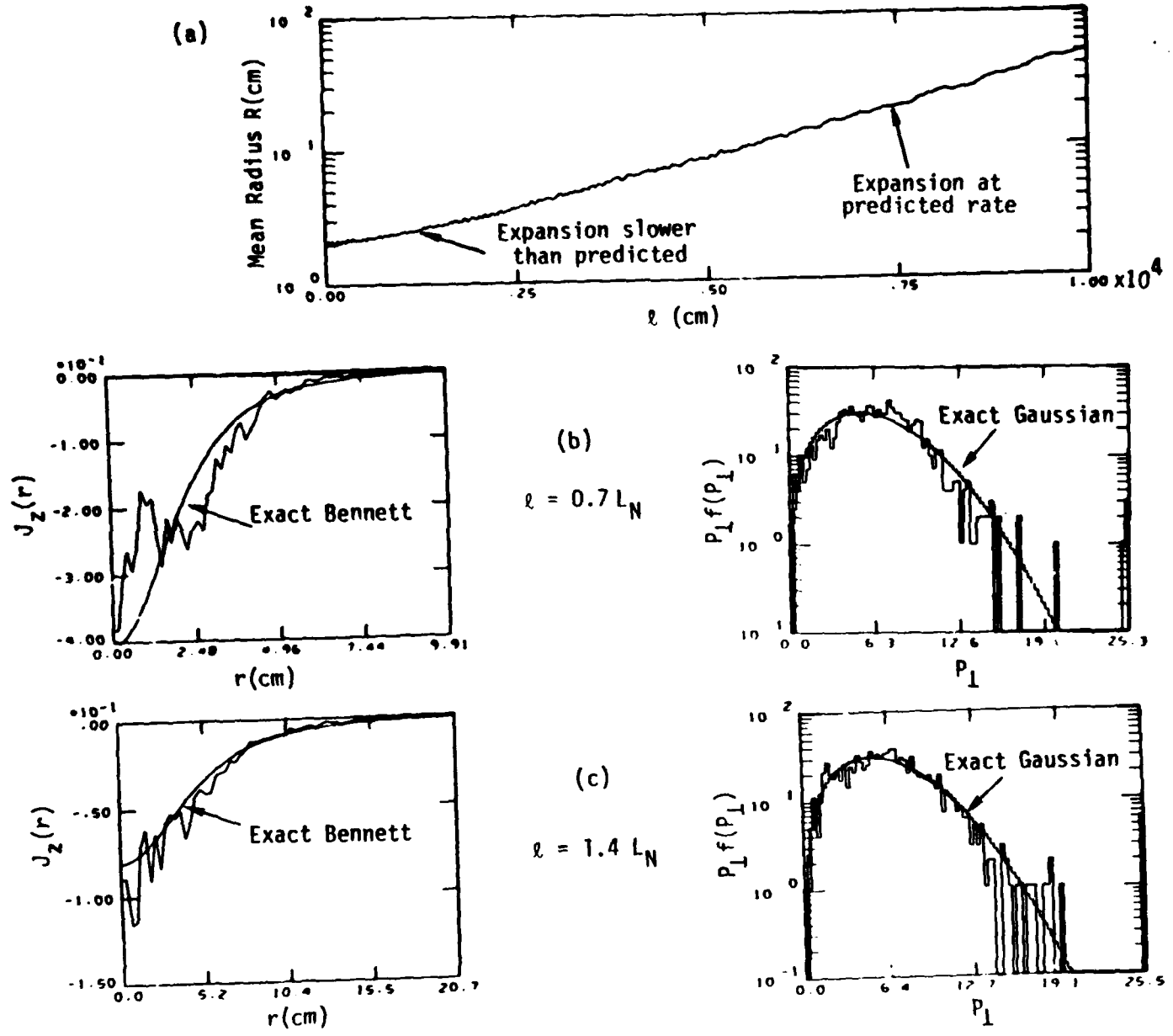

Figure 8. Evolution of the annular beam in Fig. 7 due to small angle scattering, showing the development of a Bennett profile.